

RESEARCH ARTICLE

Ontogeny and morphometrics of the gills and swim bladder of air-breathing striped catfish *Pangasianodon hypophthalmus*

Le My Phuong^{1,2}, Do Thi Thanh Huong², Hans Malte¹, Jens Randel Nyengaard³ and Mark Bayley^{1,*}

ABSTRACT

The air-breathing fish *Pangasianodon hypophthalmus* has been shown to have highly plastic branchial surfaces whose area (SA) increases with temperature and aquatic hypoxia. This modulation occurs through development of inter-lamellar cell mass (ILCM). Paradoxically, in conditions where this fish has been shown capable of covering its entire aerobic scope from the water phase, it has been shown to have a very small branchial SA. To address this paradox, we measured the SA, harmonic mean diffusion distance (τ_h) and calculated the anatomic diffusion factor (ADF) of the branchial and swim bladder surfaces in fish ranging from 3 to 1900 g at 27°C in normoxia. Since the lamellae were distinguishable from the ILCM, we measured the actual SA as well as the potential SA if ILCM were lost. As a result of low τ_h , *P. hypophthalmus* has a high capacity for branchial oxygen uptake with or without ILCM. Actual and potential gill ADF were 361 and 1002 cm² μm⁻¹ kg⁻¹, respectively, for a 100 g fish and the ADF of the swim bladder was found to be 308 cm² μm⁻¹ kg⁻¹. By swimming fish to exhaustion at different temperatures, we show that modulation of this SA is rapid, indicating that the apparent paradox between previous studies is eliminated. Regression analysis of log–log plots of respiratory SA in relation to body mass shows that the gill scales with mass similarly to the SA in active water-breathing fish, whereas the swim bladder scales with mass more like the mammalian lung does. This fish presents a combination of respiratory surfaces not previously seen in air-breathing fish.

KEY WORDS: Anatomic diffusion factor, Gill plasticity, *Pangasius*, Scaling, Stereology

INTRODUCTION

Morphometric analyses have demonstrated that the gill SA in water-breathing fish scale allometrically with body mass with a median exponent of 0.8, ranging from 0.6 to 1.0 (references listed in Table 4 for water-breathing fish). Much of the variation in this parameter correlates with the level of activity shown by the fish, with active fish possessing a much larger SA compared with sluggish fish (Gray, 1954; Hughes, 1966; Hughes and Morgan, 1973; Palzenberger and Pohla, 1992; Severi et al., 1997). Furthermore, both gill SA and τ_h show significant plasticity and are altered by a variety of

environmental factors, including oxygen demand, temperature, pH, toxicants and parasites (reviewed in Nilsson et al., 2012).

In air-breathing fish there is an additional source of variation in gill morphology because, while the majority of these species start life as water-breathers in the highly oxygenated surface waters of the tropical rainy season, they undergo developmental changes in the partitioning of oxygen uptake, with reductions in gill SA as oxygen uptake transfers to a variety of air-breathing structures (Graham, 1997). Air-breathing fish are divided into obligate air-breathers (which drown without access to air) where this ontogenetic change in gill structure is far advanced with very reduced adult gills, and facultative air-breathers, where the gills remain the main source of oxygen uptake in normoxic water during adulthood. A good illustration of this ontogenetic change occurs in the obligate air-breathing osteoglossiformid *Arapaima gigas*, where the fish hatch with fully exposed lamellae as water breathers but following the initiation of air-breathing at 8–9 days post hatch, gradually lose lamella SA and, by 1 kg in size, have completely lost these branchial respiratory surfaces and are entirely reliant on their air-breathing organ (Brauner et al., 2004).

The Pangasiidae are a group of recently evolved (Pouyaud et al., 2000) air-breathing siluriform catfishes inhabiting Southeast Asia. These species are also unusual among air-breathing fish in that they undergo extreme seasonal migration, covering at least 2000 km along the Mekong River between their spawning and feeding grounds (Van Zalinge et al., 2002). Thus, adults migrate upstream to spawn between Kratie in Cambodia and the Khone Falls of Laos (Van Zalinge et al., 2002; So et al., 2006). After spawning, adults return to their feeding grounds downstream in the floodplains of central and southern Cambodia and the Vietnamese Mekong delta, and their fingerlings drift passively in the water currents to the same areas for grow-out (Van Zalinge et al., 2002; So et al., 2006). This migration requires the species to adapt to a wide variety of environmental variables, including changes in water temperature, oxygen levels and predation risks encountered along their hazardous journey (Lucas and Baras, 2008; Li et al., 2013). While the whole migration range is tropical, water temperatures vary from around 24°C in the spawning grounds in northern Laos to a maximum of 32°C in the growth habitats of the Mekong river delta (Li et al., 2013). Recently, it has been shown that this species has strongly plastic branchial surfaces affected by both water oxygenation and water temperature (Phuong et al., 2017). Also, it has been documented that the swim bladder is highly vascularized and appears well adapted for air-breathing (Browman and Kramer, 1985; Zheng and Liu, 1988; Liu, 1993; Graham, 1997). Phuong et al. (2017) showed that the respiratory SA of the gills in *P. hypophthalmus* can be very large when respiratory lamellae are fully exposed, but that when ILCM is fully developed, they become very small and present a branchial SA consisting solely of the tips of the lamellae. The latter was the case with fish at 27°C in normoxia, while the former was the case in hypoxic 33°C water.

¹Zoophysiology Section, Department of Bioscience, Aarhus University, Denmark.

²Department of Aquatic Nutrition and Products Processing, College of Aquaculture and Fisheries, Can Tho University, 900000 Can Tho City, Vietnam. ³Core Center for Molecular Morphology, Section for Stereology and Microscopy, Department of Clinical Medicine, Centre for Stochastic Geometry and Advanced Bioimaging, Aarhus University, 8000 Aarhus C, Denmark.

*Author for correspondence (mark.bayley@bios.au.dk)

© L.M.P., 0000-0003-4986-9754; D.T.T.H., 0000-0002-9610-8467; H.M., 0000-0003-3460-1819; J.R.N., 0000-0002-8084-4646; M.B., 0000-0001-8052-2551

List of symbols and abbreviations

ABO	air-breathing organ
ADF	anatomic diffusion factor
BL	body length
CB	capillary bed
CE	coefficient of error
CV	coefficient of variance
ILCM	inter-lamellar cell mass
l_h	harmonic mean of orthogonal intercept length
M_b	body mass
SA	surface area
SA_L	lamellar surface area
SB	swim bladder
SURS	systematic uniform random sampling
TSB	swim bladder tissue
U_{crit}	critical swimming speed
U_{swim}	swimming speed
V_{air}	volume of air-space
V_F	volume of gill filament
V_L	volume of lamellae exposed to water
VUR	vertical uniform random sections
τ_h	harmonic mean diffusion distance

This represents a paradox, because Lefevre et al. (2011, 2013) showed very clearly that this species was able to meet its entire oxygen requirements from the water-phase alone in 27°C normoxic water and concluded therefore that the gills must be very large, which is unusual for an air-breathing fish with such a well-developed air-breathing organ.

The primary aim of this study was to elucidate this paradox. We therefore investigated the ontogeny of the respiratory SA of the gills and swim bladder of *P. hypophthalmus* varying in mass from ~3 g to 1900 g, in addition to the harmonic mean diffusion distance (τ_h) of these organs using vertical uniform random section (VURS)-based stereology methods. We also used these metrics to measure the anatomic diffusion factor and compared this with the literature. Finally, we tested the hypothesis that changes in activity level would stimulate a rapid increase in branchial SA by measuring the gill metrics of a group of fish where half were allowed to swim spontaneously in a growth tank, whereas the other half underwent a swimming protocol in a swim respirometer.

MATERIALS AND METHODS**Fish**

Five groups of healthy *Pangasianodon hypophthalmus* Sauvage 1878, 4.5±0.8 g ($n=6$), 24.3±0.7 g ($n=6$), 276±19 g ($n=6$), 703±41 g ($n=4$) and 1760±160 g ($n=2$) were selected from aquaria of the College of Aquaculture and Fisheries, Can Tho University (Vietnam). These fish were maintained in a 2000 litre tank at 27°C and more than 92% air saturation in clean water for 1 month. They were fed daily with commercial pellets and fasted for 2 days before organ sampling. The fish were anaesthetized in Benzocaine (1.5 g l⁻¹), killed by severing their spinal chord and their entire gills removed and immersed in 4% phosphate-buffered formalin. The swim bladders were also carefully dissected out of the fish abdomen and filled with the buffered fixative through their glottis before immersion in the same fixative for subsequent processing for stereological analysis (Fig. 1A).

Gills

The left or right gill basket was randomly chosen for analysis. The gill basket was removed from the fixative and the four gill arches

carefully dissected away from the cartilage. These were gently dried on filter paper and their individual masses noted. The entire filament tissue from the first gill arch was then processed for stereology. Before processing and embedding, the gill tissues were subsampled using a smooth fractionator and systematic uniform random sampling (SURS) with a sampling fraction of one-third or one-quarter, depending on the size of the gills (Gundersen et al., 1988; Gundersen, 2002). These chosen tissues of gill filaments (after subsampling) were then dehydrated in a graded alcohol series and infiltrated with a series of methyl methacrylate Technovit 7100 solutions (Heraeus Kulzer, Germany) before final embedding. The procedures for embedding and sectioning followed the designs of de Moraes et al. (2005) and da Costa et al. (2007), applying VURS (Baddeley et al., 1986). Ten vertical sections of 3 µm thickness were taken from each fish. These sections were stained with Haematoxylin and Eosin and analysed for stereological morphometric observation. Histological sections were then analysed using newCast stereological software VIS (Olympus, Denmark).

Swim bladder

The entire fixed swim bladder was sectioned using SURS into 5 mm slices (Fig. 1B) following the procedure of de Moraes et al. (2005). The Cavalieri principle was used to estimate the volume of swim bladder (V_{SB}) following the procedure described in Gundersen et al. (1988). These slices were then subsampled using SURS to produce 10 sampling tissues in total for embedding for light microscopy. The procedures for processing, embedding, and sectioning of these subsamples were performed using VUR principles, in the same way as for gills (described in detail in de Moraes et al., 2005).

Estimation of reference volumes, respiratory SA and τ_h

Reference volumes of gill filaments, total volume of lamellae, volume of lamellae exposed to water, volume of swim bladder tissue and volume of capillary bed in swim bladder, were determined using the Cavalieri principle (Gundersen et al., 1988; Howard and Reed, 1998; Michel and Cruz Orive, 1988). Potential lamellae SA (including parts of lamellae embedded by ILCM as well as parts exposed to water), lamellae SA (only parts exposed to water), and capillary bed SA in swim bladder were estimated using point and intersection counts of lines hitting the outer surface of the lamellae and capillary bed in swim bladder (Gundersen et al., 1988; Howard and Reed, 1998). The τ_h on lamellae and swim bladder capillary bed were determined from orthogonal intercepts based on Jensen et al. (1979). The total gill SA was calculated by multiplying the first gill arch SA by the total mass of all four gill arches and dividing by the first gill arch mass. This value was then multiplied by 2 for the whole fish. Phuong et al. (2017) showed that gill arch mass and gill SA (without ILCM) correlates well (see Fig. S1). Furthermore, it was found that there was no systematic difference between gill arches with respect to ILCM growth or τ_h .

Swimming experiment

Two size groups of 20 healthy fish (50.1±1.0 g; 18.6±0.2 cm) were also selected from aquaria of the College of Aquaculture and Fisheries, Can Tho University and acclimated in two 1500 litre tanks at 27°C and 33°C under normoxic conditions (more than 92% air saturation) for 1 month. Gills of six fish (control groups) in each tank were sampled. The gill samples were fixed and processed for stereology as described above.

The remaining fish were prepared for the swimming experiment. Each fish from the two treatments ($n=6$) was placed in the swimming respirometer (Loligo Systems, Tjele, Denmark;

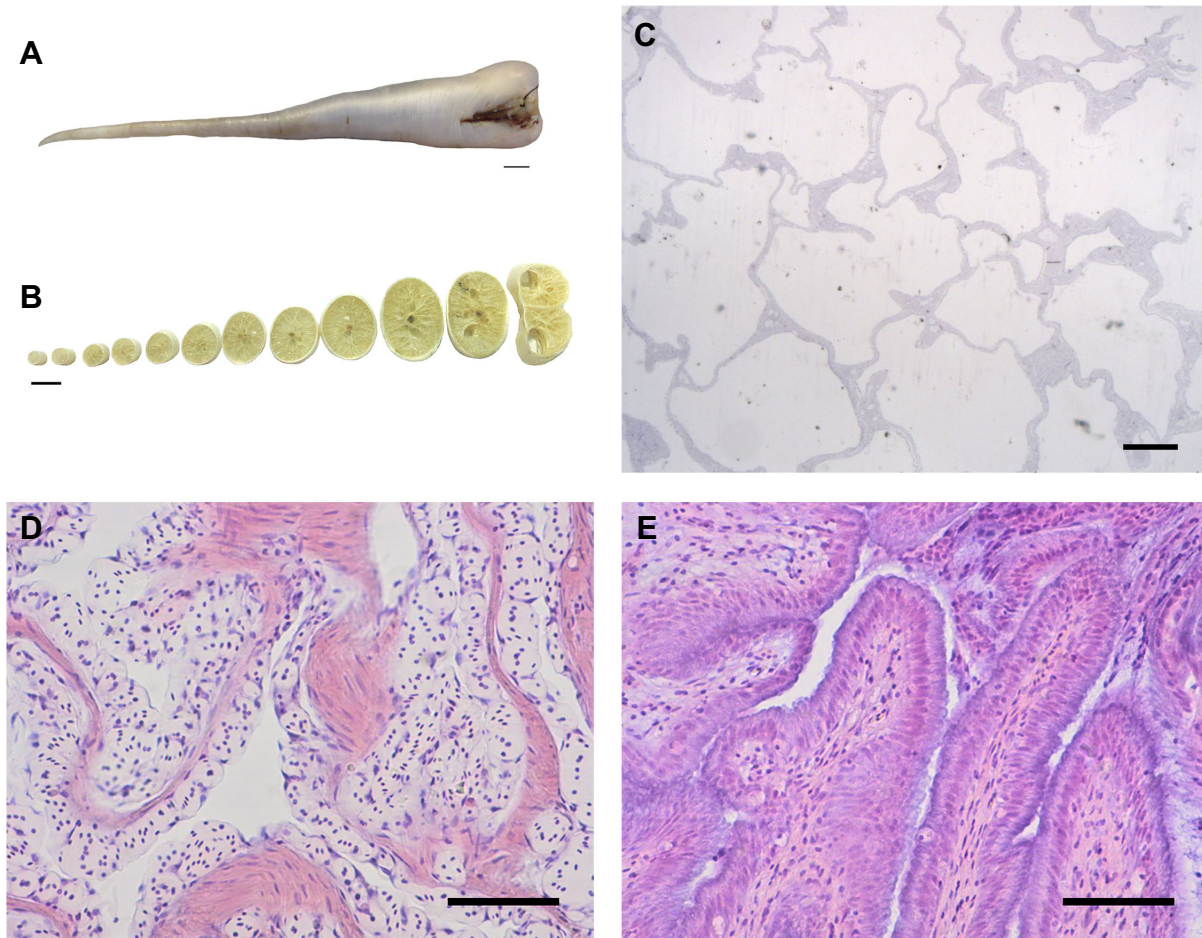


Fig. 1. Histology of the swim bladder in *Pangasianodon hypophthalmus*. (A) Entire fixed swim bladder. (B) Swim bladder slices (5 mm thickness) prepared for systematic uniform random sampling (SURS). (C) Parenchyma of the swim bladder. (D) The highly vascularized respiratory epithelium. (E) Brush border epithelium. Scale bars: 1 cm (A,B), 500 μm (C), 50 μm (D,E).

described in detail in Lefevre et al., 2013) for 16 h. During this period, the U_{swim} was maintained at 1 body length per second (1 BL s^{-1}) after which, water speed was increased by 1 BL every hour following the procedure of Lefevre et al. (2013). Water and air in the swimming chamber were renewed automatically. In addition, temperature and oxygen levels in the respirometer were controlled at the same level as the acclimation conditions. The experiment was ended when the fish was unable to remove itself from the grid for 5 s. The fish was then removed from the swimming respirometer and its gills sampled and processed for stereology as described above.

Calculations

Total volumes (all in mm^3) of gill filaments from the first gill arch [$V_{\text{F}(1\text{st})}$], volume of swim bladder tissue (V_{TSB}), volume of lamella [$V_{\text{L}(1\text{st})}$], volume of capillary bed in swim bladder (V_{CB}) and volume of air-space in swim bladder (V_{air}) were calculated using:

$$V_{\text{F}(1\text{st}),\text{TSB}} = \frac{1}{\text{TSF}} \times \frac{1}{\text{SSF}} \times \frac{1}{\text{ASF}} \times \bar{t} \times \left(\frac{A}{P}\right) \times \sum P_{\text{F}(1\text{st}),\text{TSB}}, \quad (1)$$

$$V_{\text{L}(1\text{st}),\text{CB}} = \frac{1}{\text{TSF}} \times \frac{1}{\text{SSF}} \times \frac{1}{\text{ASF}} \times \bar{t} \times \left(\frac{a}{p}\right) \times \sum P_{\text{L}(1\text{st}),\text{CB}}, \quad (2)$$

where TSF is tissue sampling fraction, SSF is section sampling fraction, ASF is area sampling fraction, t is section thickness, A/P is area per point, a/p is area per point, $\sum P_{\text{F}(1\text{st}),\text{TSB}}$ are total number of points hitting gill filaments/tissue of swim bladder, respectively, and $\sum P_{\text{L}(1\text{st}),\text{CB}}$ is total number of points hitting lamellae/capillary bed.

Total volume of gill filaments from 8 gill arches [$V_{\text{F}(\text{Total})}$] (mm^3) was calculated using:

$$V_{\text{F}(\text{Total})} = 2 \times \frac{V_{\text{F}(1\text{st})} \times \sum \text{gill arch mass}(1-4)}{\text{1st gill arch mass}}. \quad (3)$$

Volume of air in the swim bladder was calculated using $V_{\text{air}} = V_{\text{SB}} - V_{\text{TSB}}$, where V_{SB} is total volume of swim bladder (including tissue and air inside). Lamellar SA of the first gill arch and swim bladder [$\text{SA}_{\text{L}(1\text{st}),\text{SB}}$] was calculated with:

$$\text{SA}_{\text{L}(1\text{st}),\text{SB}} = 2 \times \frac{\sum I_i}{\left(\frac{l}{p}\right) \times \sum P_i} \times V_{\text{L}(1\text{st})}, \quad (4)$$

where $\sum I_i$ is total number of intersections between cycloids and lamellae/capillary bed, $\sum P_i$ is total number of points hitting

lamellae/capillary bed and l/p is length per point, and $V_{L(1st)}$ is volume of first gill arch. τ_h of the lamellae/capillary bed is $\tau_h=3/8 \times \pi \times l_h$, where l_h is harmonic mean of orthogonal intercept length of the lamellae/capillary bed. ADF of gill and swim bladder is $ADF=SA_{L(Total),SB}/\tau_h$.

The precision of the Cavalieri reference volume was estimated using the coefficient of error (CE):

$$CE(\sum P) = \frac{\sqrt{\text{Total variance of } \sum P}}{\sum P}, \quad (5)$$

$$\text{Total variance of } \sum P = \text{Noise} + \text{Var}_{\text{SURS}}(\sum \text{area}), \quad (6)$$

$$\text{Noise} = 0.0724 \times (b/\sqrt{a}) \times \sqrt{n \times \sum P}, \quad (7)$$

$$\text{Var}_{\text{SURS}}(\sum \text{area}) = \frac{3(A - \text{Noise}) - 4B + C}{240}, \quad (8)$$

with $A=P_i \times P_i$; $B=P_i \times P_{i+1}$; $C=P_i \times P_{i+2}$; mean $CE=[(CE_1^2+CE_2^2+\dots+CE_n^2)/n]^{1/2}$ and $CV=s.d./\text{mean}$. Noise is the point counting error variance, b/\sqrt{a} is the average profile shape of the observed tissues according to the nomogram of Gundersen and Jensen (1987), n is the number of examined sections, $\sum P$ is the total number of points hitting the observed tissue, $\text{Var}_{\text{SURS}}(\sum \text{area})$ is variance of the total SA and CV is the coefficient of variance.

Statistics

Data are presented as means \pm s.e.m. One-way ANOVA and Tukey's *post hoc* test were applied to compare means between the gill arch masses. Two-way ANOVA was applied to test whether swimming and/or temperatures significantly affected gill SA, τ_h and ADF; Tukey's *post hoc* test was then used to identify significant differences between fish gill SA across treatments. A probability (P) value of less than 0.05 was considered as significant. A linear regression analysis was applied to determine the relationships between logarithm data of morphometric parameters and fish body mass. These relationships are presented according to the allometric equation $Y=a(M_b)^b$ where Y is the morphometric parameter, M_b is body mass and b is the allometric exponent (the slope of the regression line in a log Y versus log M_b plot). Thus, a represents the value of the morphometric parameter at one body mass unit. These statistics were performed using PASW Statistic 18.0.

RESULTS

General structure of respiratory organs

Gills

The gills of striped catfish *P. hypophthalmus* are similar in layout to other active water-breathing teleosts, with four gill arches on each side of the head. Each gill arch includes anterior and posterior hemibranches connected with a gill raker. Lamellae are distributed along the length of the filaments from both their sides, and consist of two epithelial layers separated by pillar cells forming a sheet through which the blood flows.

Swim bladder

The swim bladder of *P. hypophthalmus* extends along the body ventral cavity from the posterior part of the head to the tail region beyond the anus. It is a single chamber, wide from the anterior part but gradually tapering to a point at the end of the coelom (Fig. 1A, B). There is a strong correlation between swim bladder length and body mass; their log–log plot gave a straight line with the slope (b) of 0.5 (r^2 , 0.98) (Table 1). The supporting structure of the swim bladder consists of collagenic fibrous walls forming subdivisions,

Table 1. Relationship between M_b and morphometrics (Y) of respiratory organs of *Pangasianodon hypophthalmus* according to the allometric equation $Y=a(M_b)^b$

Morphometric parameter (Y)	Unit	Equation	Correlation coefficient (r)
Gills			
Respiratory lamellar SA	mm ²	$Y=99.98M_b^{0.833}$	0.78
Potential respiratory lamellar SA	mm ²	$Y=215.43M_b^{0.919}$	0.87
Gill filament volume	mm ³	$Y=6.39M_b^{1.0416}$	0.94
Gill filament mass from the 1st gill arch	g	$Y=0.0016M_b^{1.097}$	0.98
Gill filament mass from the 2nd gill arch	g	$Y=0.0013M_b^{1.098}$	0.99
Gill filament mass from the 3rd gill arch	g	$Y=0.0016M_b^{1.098}$	0.99
Gill filament mass from the 4th gill arch	g	$Y=0.0012M_b^{1.068}$	0.99
Swim bladder			
Respiratory swim bladder SA	mm ²	$Y=117.17M_b^{0.714}$	0.94
Volume of swim bladder	mm ³	$Y=5.441M_b^{1.357}$	0.97
Volume of air in swim bladder	mm ³	$Y=2.141M_b^{1.482}$	0.97
Volume of capillary bed	mm ³	$Y=1.924M_b^{0.7192}$	0.90
Swim bladder length	mm	$Y=6.99M_b^{0.496}$	0.98

which contain air (Fig. 1C,D). The surfaces of the walls inside the swim bladder are covered by two types of epithelium. The first covering most of the surface is a thin respiratory type (thickness: 0.7–2.3 μm) and highly vascularized epithelium identified by the presence of red blood cells, making a capillary network where the gas exchange between blood and air in the swim bladder occurs (Fig. 1D). The second type is thick (5–15 μm) with a brush border (Fig. 1E). These two surface types are spread throughout the ABO and no discernible spatial organisation was evident.

Morphometrics of respiratory organs and relationship between these morphometrics and body mass

The morphometrics of the gills and swim bladders at different growth stages of *P. hypophthalmus* and the relationship between these parameters to fish mass are summarised in Tables 1 and 2.

Gills

The total potential respiratory SA of the lamellae (SA_L) and the SA of lamellae unblocked by ILCM are shown in Table 2. The mass of gill filament from each gill arch correlated strongly with fish M_b (r^2 , 0.99), and scaled with body size with slopes from 1.068 to 1.098 (Table 1). In all fish, the 1st and 3rd gill arches were slightly larger than those of gill arches 2 and 4 (Fig. 2; $P<0.05$). Regression analysis of log–log plots of total respiratory SA_L to body mass revealed slopes of 0.83 and 0.92, respectively, for actual and potential values (Fig. 3; Table 1). The τ_h was between 1.5 and 2.2 μm (Table 2). The ADF value of potential SA_L for a 100 g fish was 1002.4 $\text{cm}^2 \mu\text{m}^{-1} \text{kg}^{-1}$, which is three times higher than that of the actual SA_L at 361.3 $\text{cm}^2 \mu\text{m}^{-1} \text{kg}^{-1}$ for the same size fish (Table 3).

Swim bladder

There was a strong correlation between respiratory SA of swim bladder and M_b . On a log–log plot the scaling coefficient was 0.71 (r^2 , 0.94) (Fig. 4A; Table 1). The total volume of swim bladders ranged from 9 to 85 $\text{mm}^3 \text{g}^{-1}$ where air accounted for between 50 and 94% of this volume and a tendency for the air space fraction to

Table 2. Respiratory parameters in lamellae and swim bladders at different developmental stages of *Pangasianodon hypophthalmus*

Group	M_b (g)	Gills					Swim bladder								
		Respiratory SA_L/M_b ($mm^2 g^{-1}$)	Potential respiratory SA_L/M_b ($mm^2 g^{-1}$)	τ_h (μm)	CV	V_f/M_b ($mm^3 g^{-1}$)	Mean CE (%)	% Lamellae volume (V_L/V_F) $\times 100$	Respiratory SA/M_b ($mm^2 g^{-1}$)	τ_h (μm)	CV	ΣSB volume/mass ($mm^3 g^{-1}$)	%SB volume/mass	Mean CE (%)	% Air volume/ ΣSB volume
A	4.5	201.2 \pm 32.1	391.4 \pm 71.6	2.10	0.15	10.0 \pm 1.6	0.25	15.2 \pm 2.1	84.5 \pm 16.7	1.17	0.21	13.0 \pm 1.9	1.1 \pm 0.3	0.01	49.4 \pm 4.7
(n=6)	± 0.8			± 0.14						± 0.10					
B	24.3	20.0 \pm 7.4	87.5 \pm 20.8	2.16	0.08	6.3 \pm 1.3	0.08	2.2 \pm 0.6	47.3 \pm 3.1	0.82	0.08	9.3 \pm 0.8	1.0 \pm 0.1	0.01	50.3 \pm 2.4
(n=6)	± 0.7			± 0.07						± 0.03					
C	276	30.2 \pm 5.7	113.9 \pm 28.0	2.11	0.10	5.2 \pm 0.9	0.05	8.5 \pm 1.8	22.5 \pm 3.5	0.72	0.03	40 \pm 2.8	4.0 \pm 0.3	0.01	94.2 \pm 1
(n=5)	± 19			± 0.08						± 0.01					
D	703	73.3 \pm 27.1	221.2 \pm 21.8	1.53	0.26	12.2 \pm 2.2	0.01	11.0 \pm 1.0	28.1 \pm 7.0	1.85	0.57	84.6 \pm 14.7	8.5 \pm 1.5	0.03	87.5 \pm 1.7
(n=4)	± 41			± 0.20						± 0.52					
E	1760	47.4 \pm 24.0	140.0 \pm 31.1	1.65	0.32	15.8 \pm 2.7	0.01	5.7 \pm 3.1	10.2 \pm 1.6	2.26	0.28	57.8 \pm 8.1	5.8 \pm 0.8	0.01	82.7 \pm 2.7
(n=2)	± 160			± 0.37						± 0.45					

Data are presented as means \pm s.e.m.

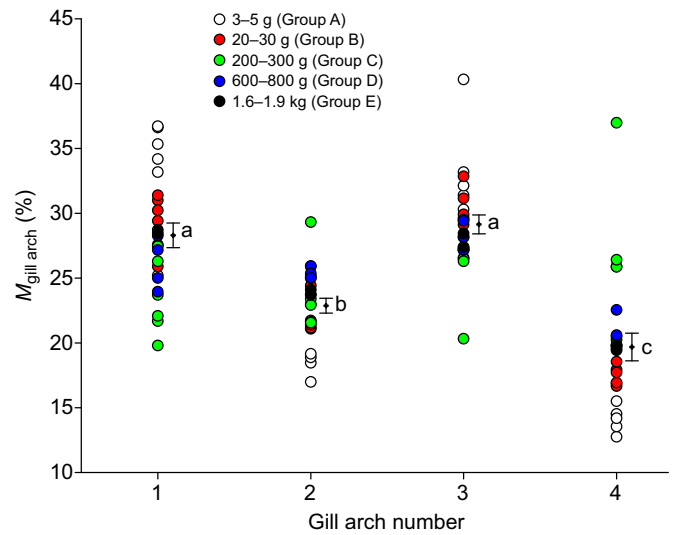


Fig. 2. Relative mass of the four gill arches expressed as a percentage of total in fish with a range of M_b . Arches 2 and 4 were significantly smaller than 1 and 3 ($P < 0.05$; One-way ANOVA and Tukey's *post hoc* test). Mean and s.e.m. for each arch are shown next to the individual data from different size groups. Different letters indicate significant differences. Fish were grouped according to mass as shown in the key.

increase with M_b (Table 2). Both the total ABO volume and the air volume of the ABO were highly correlated with M_b ; the r^2 values exceeded 0.97 and the slope b gained from the regression lines were 1.4 and 1.5, respectively (Fig. 4B; Table 1). The τ_h of the swim bladder was in the range of 0.7 to 2.3 μm (Table 2). The ADF was 308 $cm^2 \mu m^{-1} kg^{-1}$ so the apparent contribution of this organ to the total diffusing capacity in *P. hypophthalmus* at 27°C and in normoxia is ~46% (Table 3). The resistance to diffusion in the boundary layers of respiratory surfaces is, however, much more significant in water than in air and, indeed, mathematical models point out that this resistance contributes substantially to the total

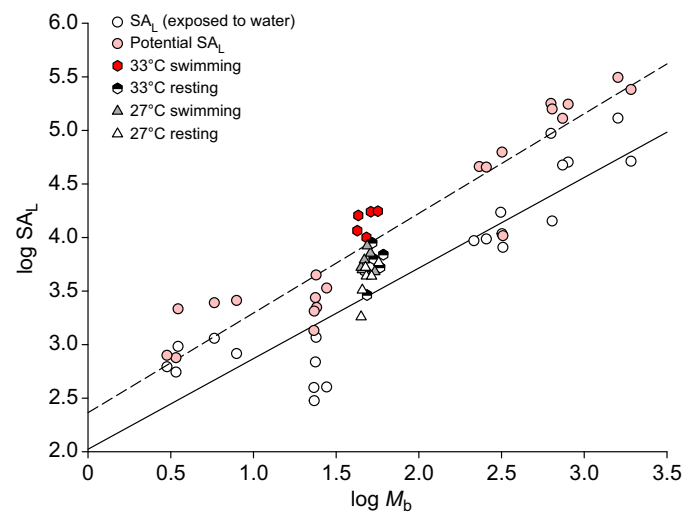


Fig. 3. Bi-logarithmic plots of lamellar SA (SA_L) in relation to M_b of *Pangasianodon hypophthalmus*. The solid regression line shows the relationship between the respiratory lamellar SA (parts of lamellae exposed to water) and M_b , with $Y=0.833X+1.999$ and $R^2=0.776$; the dashed regression line shows the relationship between the potential respiratory lamellar SA and body mass, with $Y=0.919X+2.333$ and $R^2=0.873$.

Table 3. Anatomic diffusion factor (ADF) of gills and ABOs of different fish species at the same size (100 g)

	Gills			Type	ABO			References
	τ_h (μm)	ADF ($\text{cm}^2 \mu\text{m}^{-1} \text{kg}^{-1}$)	% of total ADF		τ_h (μm)	ADF ($\text{cm}^2 \mu\text{m}^{-1} \text{kg}^{-1}$)	% of total ADF	
<i>Chaenocephalus aceratus</i>	6	200.00	100.00	–	–	–	–	Hughes (1972)
<i>Hoplias malabaricus</i>	3.16	759.49	100.00	–	–	–	–	Fernandes et al. (1994)
<i>Oncorhynchus mykiss</i>	6	400.00	100.00	–	–	–	–	Hughes (1972)
<i>Tinca tinca</i>	3	833.33	100.00	–	–	–	–	Hughes (1972)
<i>Anabas testudineus</i>	10	47.20	2.43	Sc	0.21	371.43	19.12	Hughes et al. (1973)
				Lo	0.21	1523.81	78.45	
<i>Arapaima gigas</i>	9.61	81.17	0.82	Sb	0.22	9863.64	99.18	Fernandes et al. (2012)
<i>Channa punctatus</i>	2.03	354.68	41.37	As	0.78	502.56	58.63	Hughes and Munshi (1973)
<i>Boleophthalmus boddarti</i>	1.43	517.48	90.80	Oc	1.22	52.46	9.20	Niva and Ojha (1981)
<i>Heteropneustes fossilis</i>	3.58	156.42	42.44	Sk	98	20.27	5.50	Hughes and Munshi (1973)
				As	1.6	191.88	52.06	Hughes et al. (1974)
<i>Lepidosiren paradoxa</i>	80	0.05	0.00	L	1.56	3357.05	99.80	de Moraes et al. (2005)
				Sk	161.7	6.83	0.20	
<i>Pangasianodon hypophthalmus</i>								
Actual	1.97	361.27	53.97	Sb	1.35	308.10	46.03	Present study
Potential	1.97	1002.38	76.49*	Sb	1.35	308.10	23.51*	Present study

As, air sac; Sk, skin; Sc, suprabranchial chamber; Sb, swim bladder; L, lung; St, stomach; Oc, opercular chamber; Gf, gill fans; Ao, arborescent organ; Lo, labyrinth organ.

*ADF of swim bladder was assumed not to be changed.

resistance to diffusion in the fish gill (Scheid and Piiper, 1971). Therefore, the apparent relative contribution of the ABO to the total diffusing capacity of the animal is an underestimate.

Gill SA in relation to swimming performance

There were significant differences in gill morphology between fish sampled before and after swimming (Fig. 5). The fish sampled before swimming showed gills predominantly filled with ILCM in line with expectations from normoxic conditions (Fig. 5A).

Temperature alone caused a small increase in ADF mediated by a small change in SA and little change in τ_h (Fig. 5C). Swimming, however, caused a large change in τ_h and, in combination with elevated temperature, a very large change in SA, where the gills were almost emptied of ILCM (Fig. 5B,C). Thus, the ADF and SA were significantly affected by both temperature and swimming, and the interaction between temperature and swimming ($P < 0.001$ for all three). The τ_h was significantly affected only by swimming ($P < 0.001$) and with no significant interaction ($P = 0.184$).

Table 4. Results of regression analysis from dimensions of respiratory organs (Y) in relation to M_b in different fish species

Fish species	Respiratory mode	Gill SA [$Y = a(M_b)^b$]	Type of ABO	ABO (SA)	ABO (volume)	References
<i>Thunnus albacares</i>	Water	$3151M_b^{0.875}$				Muir and Hughes (1969)
<i>Coryphaena hippurus</i>	Water	$5208M_b^{0.713}$				Hughes (1969)
<i>Scomber scombrus</i>	Water	$424.1M_b^{0.997}$				Hughes (1970)
<i>Salmo gairdneri</i>	Water	$314.8M_b^{0.932}$				Hughes (1980)
<i>Tinca tinca</i>	Water	$867.2M_b^{0.698}$				Hughes (1970)
<i>Opsanus tau</i>	Water	$560.7M_b^{0.790}$				Hughes (1969)
<i>Scyliorhinus canicula</i>	Water	$262.3M_b^{0.961}$				Hughes (1970)
<i>Torpedo marmorata</i>	Water	$117.5M_b^{0.937}$				Hughes (1978)
<i>Blennius pholis</i>	Water	$424.1M_b^{0.850}$				Milton (1971)
<i>Piaractus mesopotamicus</i>	Water	$565.04M_b^{0.769}$				Severi et al. (1997)
<i>Thunnus thynnus</i>	Water	$2443.43M_b^{0.901}$				De Jager and Dekkers (1975)
<i>Hoplias malabaricus</i>	Water	$125.1M_b^{1.140}$				Fernandes et al. (1994)
<i>Micropterus dolomieu</i>	Water	$731.14M_b^{0.820}$				De Jager and Dekkers (1975)
<i>Oncorhynchus mykiss</i>	Water	$389.94M_b^{0.900}$				De Jager and Dekkers (1975)
<i>Hoplias lacerdae</i>	Water	$491.7M_b^{0.810}$				Fernandes et al. (1994)
<i>Botia lohachata</i>	Water	$913.3M_b^{0.699}$				Sharma et al. (1982)
<i>Oreochromis niloticus</i>	Water	$515.16M_b^{0.750}$				Fernandes and Rantin (1986)
<i>Ictalurus nebulosus</i>	Water	$264.85M_b^{0.845}$				De Jager and Dekkers (1975)
<i>Catostomus commersonii</i>	Water	$797.99M_b^{0.639}$				De Jager and Dekkers (1975)
<i>Macrognathus aculeatum</i>	Water	$217.3M_b^{0.733}$				Ojha and Munshi (1974)
<i>Amphipnous cuchia</i>	Water	$888.4M_b^{0.709}$				Hughes et al. (1974)
<i>Anabas testudineus</i>	Air	$556M_b^{0.615}$				Hughes and Munshi (1973)
<i>Channa punctata</i>	Air	$470.4M_b^{0.592}$	Sc	$1.591M_b^{0.696}$	$0.024M_b^{0.855}$	Hakim et al. (1978)
<i>Saccobranchus fossilis</i>	Air	$186.1M_b^{0.746}$	As	$145M_b^{0.662}$	$0.004M_b^{0.999}$	Hughes et al. (1974)
			Sk	$851.1M_b^{0.684}$		
<i>Pangasianodon hypophthalmus</i>						
Actual	Air	$99.98M_b^{0.833}$	Sb	$117.17M_b^{0.714}$	$5.441M_b^{1.357}$	Present study
Potential	Air	$215.43M_b^{0.920}$				Present study

Sc, suprabranchial chamber; As, air sac; Sk, skin; Sb, swim bladder.

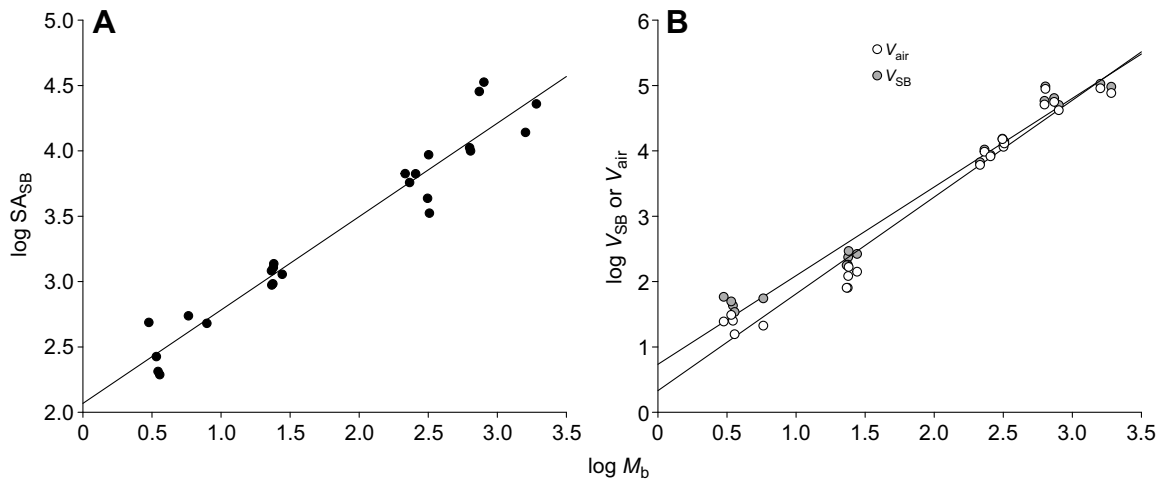


Fig. 4. Bi-logarithmic plots of swim bladder dimensions in relation to body mass of *Pangasianodon hypophthalmus*. (A) Relationship between swim bladder respiratory SA (SA_{SB}) and M_b , with regression line $Y=0.714X+2.069$ and $R^2=0.940$. (B) Relationship between total swim bladder volume (grey circles) and air-space volume in swim bladder (white circles) against M_b , with regression lines of $Y=1.357X+0.736$ and $R^2=0.973$, and $Y=1.482X+0.331$ and $R^2=0.967$, respectively.

DISCUSSION

Gill plasticity and anatomic diffusion factor (ADF)

Lefevre et al. (2011, 2013) showed that in normoxic water at 27°C, *P. hypophthalmus* did not require the air phase to cover its oxygen requirements either in a resting state or when swimming at maximum sustainable speed. On this basis, and as a result of superficial low-magnification examination of the branchial SA, the authors argued that the gills of this species are unusually large for an air-breathing fish. In contrast to this, Phuong et al. (2017) showed using stereological methods that under the conditions of the Lefevre et al. studies, *P. hypophthalmus* gills are in fact very small because the inter-lamellar spaces are entirely filled with cell mass, presenting a difficult paradox of how branchial oxygen uptake can be achieved in such an active tropical fish. Gill SA is important in gas exchange, but examining gill SA alone is insufficient for evaluation of oxygen uptake capacity. The τ_h is equally important because diffusion capacity is proportional to the respiratory gill area and inversely proportional to τ_h (Hughes, 1972; Hughes and Morgan, 1973). These two parameters can be conveniently combined to calculate the ADF, which represents the anatomical component of the diffusion capacity of the particular respiratory SA (Perry, 1978). This allows an evaluation of the relative importance of the respiratory SA in this species under different conditions as well as a more informed comparison with other species. The gill SA in 27°C normoxic water in the present study was strongly reduced by ILCM (Table 2), which is in agreement with Phuong et al. (2017). However, both studies show that this species presents an unusually thin diffusion barrier between the water and the blood (Table 3). The result of this is that even with ILCM, the gills still present a relatively large ADF (361.3 cm² μm⁻¹ kg⁻¹ for a 100 g fish), which is similar to active water-breathers such as trout. When fully exposed by removal of ILCM, the gills show a higher ADF (1002 cm² μm⁻¹ kg⁻¹ for a 100 g fish) compared with that in most water-breathers and significantly higher than for other air-breathing fish (Table 3). In addition, at 27°C, *P. hypophthalmus* haemoglobin has a rather strong oxygen affinity with a P_{50} of 4.6 torr (calculated from Damsgaard et al., 2015a). At higher oxygen demands, at elevated temperatures or via swimming, *P. hypophthalmus* can increase the diffusion capacity of its branchial

SA by reduction of ILCM. It should be noted when making this inter-species comparison that the habitat temperature for *P. hypophthalmus* is significantly higher than most species in this branchial ADF comparison. However, the present study strongly indicates that even with ILCM this species should probably be able to sustain a standard metabolic rate from the water alone. Should the need for more oxygen arise, for example as a result of exhaustive swimming as in Lefevre et al. (2013), the present study shows that the SA can change rapidly (Fig. 5). Hence, the paradox presented in this fish is resolved.

Relative importance of the ABO and the osmo-respiratory compromise

The ABO of a 100 g *P. hypophthalmus* accounts for between 50% of the animal's total ADF, when gills are filled with ILCM, decreasing to <25% when the gills are fully exposed to the water (Table 3). Examination of data in Table 3 reveals that this value is typical of the facultative air-breathing fish examined to date. Interestingly, while the ABO accounts for only 25–50% of the total, this organ can support this at the industrial scale production in deeply hypoxic Vietnamese growth ponds (Damsgaard et al., 2015b, supplementary data), although the available growth data from controlled laboratory environments show improved growth in normoxic water (Lefevre et al., 2014; Phuong et al., 2017). The ability to obtain oxygen from both aquatic and aerial source has surely conferred an adaptive advantage in organically rich tropical water where hypoxia is a regularly recurring event (Johansen, 1968; Johansen et al., 1970). However, the question remains as to why a fish reduces its branchial ADF in normoxic water. It has previously been argued that branchial reductions might serve to reduce branchial loss of oxygen obtained from the surface in hypoxic water (Randall et al., 1981), but in pangasius this does not seem to hold true with the largest branchial SA in high-temperature hypoxia and the smallest in low-temperature normoxia. Perhaps a more likely explanation is that this fish provides positive evidence of the trade-off between the requirement for a thin respiratory epithelium to facilitate gas exchange whilst at the same time maximising the diffusion barrier for water and passive ion loss, termed the osmo-respiratory compromise (Wood and Randall, 1973a,b; Nilsson,

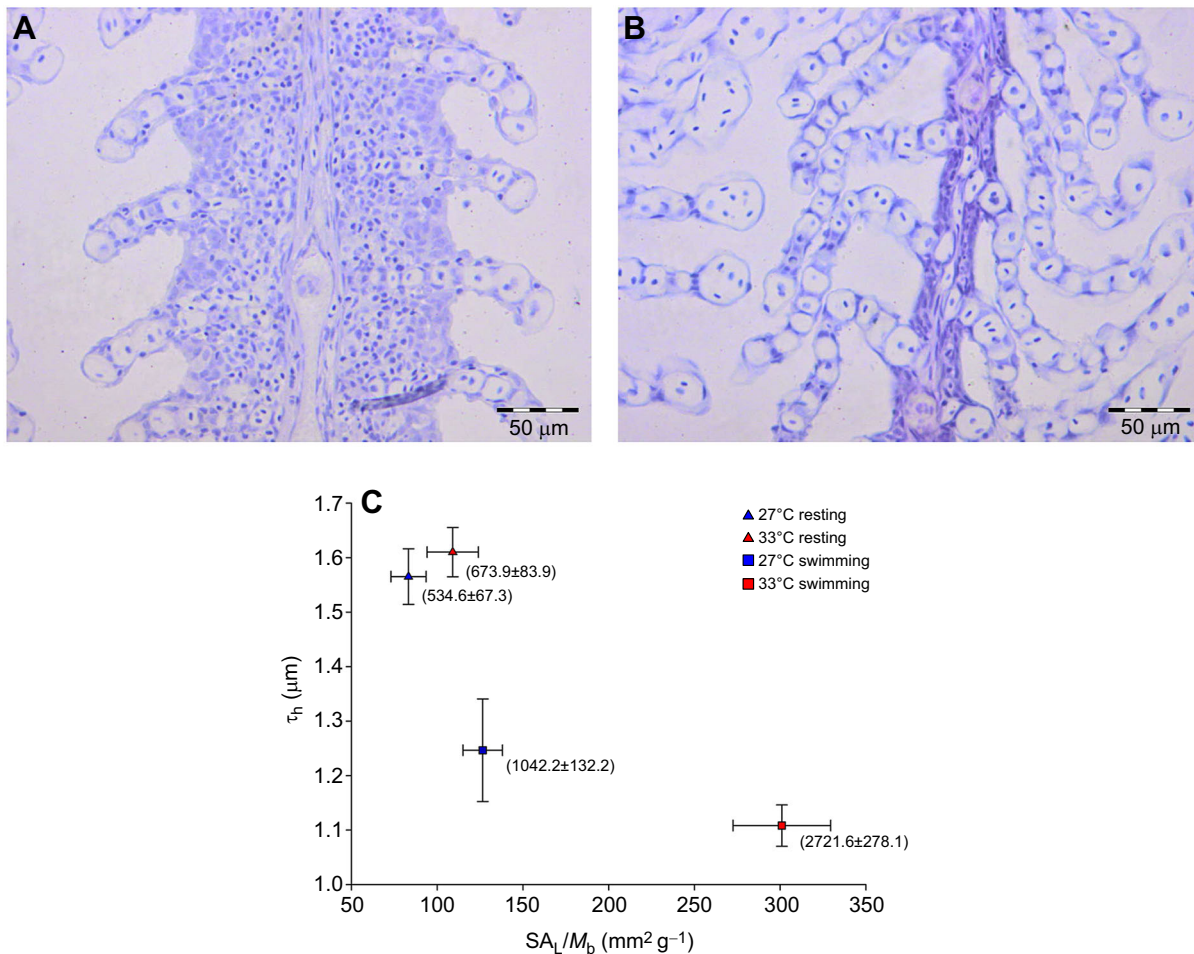


Fig. 5. Histological cross sections of gill filaments of *Pangasianodon hypophthalmus*. (A) Histology of fish exposed to a temperature of 27°C before swimming. (B) Histology of fish maintained at 33°C after swimming. (C) Respiratory lamellar SA (SA_L, corrected for mass) and τ_h of *P. hypophthalmus* induced by different temperature and swimming conditions. Numbers in brackets indicate associated gill ADF values (cm² μm⁻¹ kg⁻¹). N=6 in all groups.

1986; Gonzalez and McDonald, 1992, 1994; Nilsson, 2007). Reducing the respiratory SA by adding the ILCM barrier may help prevent ion loss or unwanted water uptake and therefore reduce ion-regulatory energy consumption. This is an area in need of further research as we could see no evidence of mitochondrial-rich cells on the lamellae in the present study, although fluorescence microscopy will be necessary to confirm this. The speed with which ILCM can be increased or reduced should be examined on a finer time scale. In addition, further work should focus on whether there are vascular shunts within the gills or whether there is some other mechanism modulating the leakiness of lamellar epithelial membrane in this species.

Relationship between morphometrics of gills and body size

It has long been known that fish gill SA in relation to M_b shows a good fit with the equation $Y=a(M_b)^b$. This relationship has been confirmed for numerous water-breathing fish and several air-breathing fish (summarized in Table 4). Much of the variation in the exponent (*b* values), has been argued to be correlated with the activity level of the species and its habitat choice (Gray, 1954; Hughes, 1966; Palzenberger and Pohla, 1992; Fernandes et al., 1994; Severi et al., 1997). In the present study, the slopes of the regression lines for the actual and potential respiratory lamellar area

against M_b were 0.83 and 0.92, respectively. These values are within the range of 0.8 to 0.9 found in active water-breathing fish species, but significantly greater than found in other air-breathing fish, such as *Anabas testudineus* (0.615), *Saccobranchius fossilis* (0.746) and *Channa punctata* (0.592) (Table 4). The high value of the slopes in *P. hypophthalmus* also correlates with the active habits of this species with its strenuous migratory pattern between Laos and the Mekong river delta, a distance of more than 2000 km (Van Zalinge et al., 2002; So et al., 2006).

It has previously been pointed out that the scaling relationship between respiratory SA and body size was similar to the relationship between oxygen consumption rates and body size in a variety of fish species, with log–log plot slopes also in the range of 0.8 to 0.9 (reviewed in Schmidt–Nielsen, 1984). However, it has been noted that these two slopes do not always match (Singh and Munshi, 1985). The argument for this mismatch has typically been that the functional SA changes dramatically with oxygen demand as a result of recruitment of lamellae (Jones and Randall, 1978; Booth, 1978; Farrell et al., 1980; Wood and Perry, 1985; Perry and Wood, 1989). In addition to lamellar recruitment changing the SA, it has also been shown that ILCM can change the functional SA. Thus, crucian carp (*Carassius carassius*) exposed to hypoxia in a closed respirometer at 20°C significantly reduced their ILCM within 6 h (Sollid et al.,

2005). This species also reduced ILCM volume by 65% within 8 h of an increase in swimming speed (Brauner et al., 2011). Similarly, the closely related goldfish (*Carassius auratus*) lost 18% of ILCM within 30 min of exposure to hypoxia at 7°C (Tzaneva et al., 2011), and Fu et al. (2011) found that exposure to hypoxia for 48 h or sustained exercise (70% of U_{crit}) induced a significant increase in lamellar SA. Perry et al. (2012) found that while the gills of goldfish acclimated to low temperature (7°C) were filled with ILCM, the SA increased by 45% after ~3 h of swimming by reducing the ILCM. Similarly in the present study we found that *P. hypophthalmus* at 27°C and normoxia have their gills partly embedded by ILCM, making their respiratory gill SA less than 30% of their maximal area. Swimming the fish for 20 h caused an increase in SA, with the effect most pronounced at 33°C where oxygen demand is highest (Fig. 5C). The mechanisms involved in these changes in ILCM are at present unclear but Nilsson et al. (2012) suggested two possible routes of ILCM removal: a slow route via increased apoptosis and decreased mitosis (Sollid et al., 2003) and a rapid route by simple shedding of ILCM cells into the water. Given the rapidity of the changes incurred during swimming in both *P. hypophthalmus* and goldfish, it is likely that simple shedding of cells occurs during these urgent increases in oxygen demand.

It is clear that the main mediator of gill ADF is the oxygen demand of the fish. Swimming has a large effect on τ_h in our study, which might be expected by increased lamella perfusion causing distension of the lamellae (Soivio and Tuurala, 1981). The temperature change alone in our study had no effect on gill τ_h but did cause a minor significant increase in gill SA. This is in line with our previous findings in this species where the same temperature increase caused only a minor effect on SA unless combined with hypoxia (Phuong et al., 2017). In the eel (*Anguilla anguilla*), a larger temperature change (7 to 25°C) was associated with a halving of the τ_h (Tuurala et al., 1998). The combined oxygen demand caused by both swimming and elevated temperature then led to both distension and hence reduction of τ_h and a massive increase in SA as a result of shedding of the entire ILCM (Fig. 5). It would be interesting to further investigate the time scale of modulation of ILCM to determine how it might match the dynamics of a shifting oxygen environment (for example in river eddies) and the energetic needs of the animal. The role of ILCM in offsetting negative costs of osmo-respiratory compromise has been discussed on numerous occasions (Nilsson et al., 2012; Perry et al., 2012; Phuong et al., 2017), but the costs of building and shedding of cell mass are presently unknown.

Air-breathing organ and body size

The air-breathing organ volumes in the present study are between 1 and 8.5% of fish volume, which is in the range found in other fish species where it has been quantified for its role in providing positive buoyancy (Alexander, 1959a,b). However, a note of caution should be raised here because of the difficulties of maintaining ABO volume during fixation. In the large fish (groups C–E; Table 2), the ABO was filled with fixative and the trachea tied off to prevent deformation of the lung type structure during fixation. It was not possible to tie the trachea in the two smallest groups (groups A,B; Table 2) hence their unusually low volumes may well be a result of some deformation during fixation. Thus the scaling coefficients for the ABO with M_b must be viewed with caution. Information on the relationship between ABO dimensions and M_b is available on very few fish species, but this has been extensively investigated in mammals and birds (reviewed in Schmidt-Nielsen, 1984). The regression line from the log-log plot of swim bladder respiratory SA

against M_b gave a slope of 0.714, which is smaller than that for gill SA (0.83 and 0.92, respectively, for actual and potential SA), but similar to the scaling of the mammalian lung (Schmidt-Nielsen, 1984).

P. hypophthalmus is in several respects unusual among air-breathing fish. It is a fast swimmer capable of the sustained exertion necessary for the >2000 km upstream migration for spawning, in itself unusual in this group. Whereas all other air-breathing fish examined previously have reduced gills compared with water-breathers, this species has adopted the alternative of maintaining large gills with thin respiratory epithelia, instead modulating the SA using ILCM, while at the same time developing a large ABO through which it can sustain itself during periods of hypoxia. This combination is at present unique among air-breathing fish. Pouyaud et al. (2000) showed that speciation in the Pangasiidae is very recent, occurring in the mid Miocene, and it is tempting to speculate that the respiratory set-up in *P. hypophthalmus* represents an early evolutionary step in the transition from water-breathing to air-breathing.

Acknowledgements

The authors would like to thank three Bachelor students Mai Hoang Anh Dung, Truong Thi Ngoc Huyen and Vo Nguyen Khanh at Can Tho University for their assistance with this study.

Competing interests

The authors declare no competing or financial interests.

Author contributions

Conceptualization: L.P., J.R.N., M.B.; Methodology: L.P., J.R.N., M.B.; Software: J.R.N.; Formal analysis: L.P., H.M., J.R.N.; Investigation: L.P.; Resources: D.H., J.R.N., M.B.; Data curation: L.P., M.B.; Writing - original draft: L.P.; Writing - review & editing: D.H., H.M., J.R.N., M.B.; Visualization: L.P., H.M., M.B.; Supervision: D.H., J.R.N., M.B.; Project administration: D.H., M.B.; Funding acquisition: D.H., M.B.

Funding

This study was funded by The Danish International Development Agency (DANIDA), Danish Ministry of Foreign Affairs, iAQUA project [DFCno. 12-014AU].

Supplementary information

Supplementary information available online at <http://jeb.biologists.org/lookup/doi/10.1242/jeb.168658.supplemental>

References

- Alexander, R. McN. (1959a). The physical properties of the swim bladder in intact Cypriniformes. *J. Exp. Biol.* **36**, 315–332.
- Alexander, R. McN. (1959b). The physical properties of the swim bladder in intact Cypriniformes. *J. Exp. Biol.* **36**, 347–355.
- Baddeley, A. J., Gundersen, H. J. G. and Cruz-Orive, L. M. (1986). Estimation of surface area from vertical sections. *J. Microsc.* **142**, 259–276.
- Booth, J. H. (1978). The distribution of blood flow in the gills of fish: application of a new technique to rainbow trout (*Salmo gairdneri*). *J. Exp. Biol.* **73**, 119–129.
- Brauner, C. J., Matey, V., Wilson, J. M., Bernier, N. J. and Val, A. L. (2004). Transition in organ function during the evolution of air-breathing: insights from *Arapaima gigas*, an obligate air-breathing teleost from the Amazon. *J. Exp. Biol.* **207**, 1433–1438.
- Brauner, C. J., Matey, V., Zhang, W., Richards, J. G., Dhillon, R., Cao, Z. D., Wang, Z. Y. and Fu, S. J. (2011). Gill remodeling in crucian carp during sustained exercise and the effect on subsequent swimming performance. *Physiol. Biochem. Zool.* **84**, 535–542.
- Browman, M. W. and Kramer, D. L. (1985). *Pangasius sutchi* (Pangasiidae), an air-breathing catfish that uses the swimbladder as an accessory respiratory organ. *Copeia* **1985**, 994–998.
- da Costa, O. T., Pedretti, A. C. E., Schmitz, A., Perry, S. F. and Fernandes, M. N. (2007). Stereological estimation of surface area and barrier thickness of fish gills in vertical sections. *J. Microsc.* **225**, 1–9.
- Damsgaard, C., Phuong, L. M., Jensen, F. B., Wang, T. and Bayley, M. (2015a). High affinity and temperature sensitivity of blood oxygen binding in *Pangasianodon hypophthalmus* due to lack of chloride-hemoglobin allosteric interaction. *Am. J. Physiol. Regul. Integr. Comp. Physiol.* **308**, R907–R915.

- Damsgaard, C., Tuong, D. D., Thinh, P. V., Wang, T. and Bayley, M.** (2015b). High capacity for extracellular acid–base regulation in the air-breathing fish *Pangasianodon hypophthalmus*. *J. Exp. Biol.* **218**, 1290–1294.
- De Jager, S. and Dekkers, W. J.** (1975). Relations between gill structure and activity in fish. *Neth. J. Zool.* **25**, 276–308.
- de Moraes, M. F. P. G., Höller, S., da Costa, O. T., Glass, M. L., Fernandes, M. N. and Perry, S. F.** (2005). Morphometric comparison of the respiratory organs in the South American lungfish *Lepidosiren paradoxa* (Dipnoi). *Physiol. Biochem. Zool.* **78**, 546–559.
- Farrell, A. P., Sobin, S. S., Randall, D. J. and Crosby, S.** (1980). Intralamellar blood flow patterns in fish gills. *Am. J. Physiol. Regul. Integr. Comp. Physiol.* **239**, R428–R436.
- Fernandes, M. N. and Rantin, F. T.** (1986). Gill morphometry of cichlid fish, *Oreochromis* (Sarotherodon) *niloticus* (Pisces, Teleostei). *Ciencia e cultura* **38**, 192–198.
- Fernandes, M. N., Rantin, F. T., Kalinin, A. L. and Moron, S. E.** (1994). Comparative study of gill dimensions of three erythrinid species in relation to their respiratory function. *Can. J. Zool.* **72**, 160–165.
- Fernandes, M. N., da Cruz, A. L., da Costa, O. T. F. and Perry, S. F.** (2012). Morphometric partitioning of the respiratory surface area and diffusion capacity of the gills and swim bladder in juvenile Amazonian air-breathing fish, *Arapaima gigas*. *Micron* **43**, 961–970.
- Fu, S.-J., Brauner, C. J., Cao, Z.-D., Richards, J. G., Peng, J.-L., Dhillon, R. and Wang, Y.-X.** (2011). The effect of acclimation to hypoxia and sustained exercise on subsequent hypoxia tolerance and swimming performance in goldfish (*Carassius auratus*). *J. Exp. Biol.* **214**, 2080–2088.
- Gonzalez, R. J. and McDonald, D. G.** (1992). The relationship between oxygen consumption and ion loss in a freshwater fish. *J. Exp. Biol.* **163**, 317–332.
- Gonzalez, R. and McDonald, D. G.** (1994). The relationship between oxygen uptake and ion loss in fish from diverse habitats. *J. Exp. Biol.* **190**, 95–108.
- Graham, J. B.** (1997). *Air-Breathing Fishes: Evolution, Diversity, and Adaptation*. San Diego: Academic Press.
- Gray, I. E.** (1954). Comparative study of the gill area of marine fishes. *Biol. Bull.* **107**, 219–225.
- Gundersen, H. J. G.** (2002). The smooth fractionator. *J. Microsc.* **207**, 191–210.
- Gundersen, H. J. G. and Jensen, E. B.** (1987). The efficiency of systematic sampling in stereology and its prediction. *J. Microsc.* **147**, 229–263.
- Gundersen, H. J. G., Bagger, P., Bendtsen, T. F., Evans, S. M., Korbo, L. X. M. N., Marcussen, N., Møller, A., Nielsen, K., Nyengaard, J. R., Pakkenberg, B. et al.** (1988). The new stereological tools: disector, fractionator, nucleator and point sampled intercepts and their use in pathological research and diagnosis. *APMIS* **96**, 857–881.
- Hakim, A., Munshi, J. S. Hughes, G. M.** (1978). Morphometries of the respiratory organs of the Indian green snake-headed fish, *Channa punctata*. *J. Zool.* **184**, 519–543.
- Howard, C. V. and Reed, M. G.** (1998). *Unbiased Stereology. Three-dimensional Measurement in Microscopy*. Oxford, U.K: Bios Scientific Publishers.
- Hughes, G. M.** (1966). The dimensions of fish gills in relation to their function. *J. Exp. Biol.* **45**, 177–195.
- Hughes, G. M.** (1969). Morphological measurements on the gills of fishes in relation to their respiratory function. *Folia Morphol.* **18**, 78–95.
- Hughes, G. M.** (1970). A comparative approach to fish respiration. *Cell. Mol. Life Sci.* **26**, 113–122.
- Hughes, G. M.** (1972). Morphometrics of fish gills. *Respir. Physiol.* **14**, 1–25.
- Hughes, G. M.** (1978). On the respiration of *Torpedo marmorata*. *J. Exp. Biol.* **73**, 85–105.
- Hughes, G. M.** (1980). Functional morphology of fish gills. In *Epithelial Transport in the Lower Vertebrates* (ed. B. Lahlou), pp. 15–36. London: Cambridge Univ Press.
- Hughes, G. M. and Morgan, M.** (1973). The structure of fish gills in relation to their respiratory function. *Biol. Rev.* **48**, 419–475.
- Hughes, G. M. and Munshi, J. S.** (1973). Nature of the air-breathing organs of the Indian fishes *Channa*, *Amphipnous*, *Clarias* and *Saccobranchus* as shown by electron microscopy. *J. Zool.* **170**, 245–270.
- Hughes, G. M., Dube, S. C. and Munshi, J. S.** (1973). Surface area of the respiratory organs of the climbing perch, *Anabas testudineus* (Pisces: Anabantidae). *J. Zool.* **170**, 227–243.
- Hughes, G. M., Singh, B. R., Thakur, R. N. and Munshi, J. S. D.** (1974). Areas of the air-breathing surfaces of *Amphipnous cuchia* (Ham.). *Proc. Natl. Acad. Sci. India* **40**, 379–392.
- Jensen, E. B., Gundersen, H. J. G. and Østerby, R.** (1979). Determination of membrane thickness distribution from orthogonal intercepts. *J. Microsc.* **115**, 19–33.
- Johansen, K.** (1968). Air-breathing fishes. *SciAm* **219**, 102–111.
- Johansen, K., Hanson, D. and Lenfant, C.** (1970). Respiration in a primitive air breather, *Amia calva*. *Resp. Physiol.* **9**, 162–174.
- Jones, D. R. and Randall, D. J.** (1978). The respiratory and circulatory system. In *“Fish Physiology”*, Vol. 7 (ed. W.S. Hoar and D. J. Randall), pp. 425. New York: Academic Press.
- Lefevre, S., Wang, T., Phuong, N. T. and Bayley, M.** (2011). Hypoxia tolerance and partitioning of bimodal respiration in the striped catfish (*Pangasianodon hypophthalmus*). *Comp. Biochem. Physiol. A.* **158**, 207–214.
- Lefevre, S., Wang, T., Huong, D. T. T., Phuong, N. T. and Bayley, M.** (2013). Partitioning of oxygen uptake and cost of surfacing during swimming in the air-breathing catfish *Pangasianodon hypophthalmus*. *J. Comp. Physiol. B.* **183**, 215–221.
- Lefevre, S., Wang, T., Jensen, A., Cong, N. V., Huong, D. T. T., Phuong, N. T. and Bayley, M.** (2014). Air-breathing fishes in aquaculture. What can we learn from physiology? *J. Fish Biol.* **84**, 705–731.
- Li, S., Lu, X. X. and Bush, R. T.** (2013). CO₂ partial pressure and CO₂ emission in the Lower Mekong River. *J. Hydrol.* **504**, 40–56.
- Liu, W. S.** (1993). Development of the respiratory swimbladder of *Pangasius sutchi*. *J. Fish Biol.* **42**, 159–167.
- Lucas, M. and Baras, E.** (2008). *Migration of Freshwater Fishes*. Oxford: Blackwell Sciences.
- Michel, R. P. and Cruz-Orive, L. M.** (1988). Application of the Cavalieri principle and vertical sections method to lung: estimation of volume and pleural surface area. *J. Microsc.* **150**, 117–136.
- Milton, P.** (1971). Oxygen consumption and osmoregulation in the shanny, *Blennius pholis*. *J. Mar. Biol. Assoc. UK* **51**, 247–265.
- Muir, B. S. and Hughes, G. M.** (1969). Gill dimensions for three species of tunny. *J. Exp. Biol.* **51**, 271–285.
- Nilsson, S.** (1986). Control of gill blood flow. In *Fish Physiology: Recent Advances* (ed. S. Nilsson and S. Holmgren), pp. 87–101. London: Croom Helm.
- Nilsson, G. E.** (2007). Gill remodeling in fish—a new fashion or an ancient secret? *J. Exp. Biol.* **210**, 2403–2409.
- Nilsson, G. E., Dymowska, A. and Stecyk, J. A.** (2012). New insights into the plasticity of gill structure. *Resp. Physiol. Neurobiol.* **184**, 214–222.
- Niva, B. and Ojha, J.** (1981). Morphometrics of the respiratory organs of an estuarine goby, *Boleophthalmus boddarti*. *Jap. J. Ichthyol.* **27**, 316–326.
- Ojha, J. and Munshi, J. S. D.** (1974). Morphometric studies of the gill and skin dimensions in relation to body weight in a fresh-water mud eel, *Macroglyptus aculeatum* (Bloch). *Zool. Anz. Jena.* **193**, 364–381.
- Palzenberger, M. and Pohla, H.** (1992). Gill surface area of water-breathing freshwater fish. *Rev. Fish Biol. Fish.* **2**, 187–216.
- Perry, S. F.** (1978). Quantitative anatomy of the lungs of the red-eared turtle, *Pseudemys scripta elegans*. *Respir. Physiol.* **35**, 245–262.
- Perry, S. F. and Wood, C. M.** (1989). Control and coordination of gas transfer in fishes. *Can. J. Zool.* **67**, 2961–2970.
- Perry, S. F., Fletcher, C., Bailey, S., Ting, J., Bradshaw, J., Tzaneva, V. and Gilmour, K. M.** (2012). The interactive effects of exercise and gill remodeling in goldfish (*Carassius auratus*). *J. Comp. Physiol. B.* **182**, 935–945.
- Phuong, L. M., Huong, D. T. T., Nyengaard, J. R. and Bayley, M.** (2017). Gill remodelling and growth rate of striped catfish *Pangasianodon hypophthalmus* under impacts of hypoxia and temperature. *Comp. Biochem. Physiol. A.* **203**, 288–296.
- Pouyau, L., Teugels, G. G., Gustiano, R. and Legendre, M.** (2000). Contribution to the phylogeny of pangasiid catfishes based on allozymes and mitochondrial DNA. *J. Fish Biol.* **56**, 1509–1538.
- Randall, D. J., Cameron, J. N., Daxboeck, C. and Smatresk, N.** (1981). Aspects of bimodal gas exchange in the bowfin: *Amia calva* L. (Actinopterygii: Amiiformes). *Respir. Physiol.* **43**, 339–348.
- Scheid, P. and Piper, J.** (1971). Theoretical analysis of respiratory gas equilibration in water passing through fish gills. *Respir. Physiol.* **13**, 305–318.
- Schmidt-Nielsen, K.** (1984). *Scaling: Why is Animal Size so Important?* Cambridge: Cambridge University Press.
- Severi, W., Rantin, F. T. and Fernandes, M. N.** (1997). Respiratory gill surface of the serrasalmid fish, *Piaractus mesopotamicus*. *J. Fish Biol.* **50**, 127–136.
- Sharma, S. N., Guha, G. and Singh, B. R.** (1982). Gill dimensions of a hillstream fish, *Botia lohachata* (Pisces, Cobitidae). *Proc. Ind. Nat. Sci. Acad. B.* **48**, 81–91.
- Singh, O. N. and Munshi, J. D.** (1985). Oxygen uptake in relation to body weight, respiratory surface area and group size in a freshwater goby, *Glossogobius giurus* (Ham.). *Proc Ind Nat. Sci. Acad. B.* **51**, 33–40.
- So, N., Van Houdt, J. K. and Volckaert, F. A.** (2006). Genetic diversity and population history of the migratory catfishes *Pangasianodon hypophthalmus* and *Pangasius bocourti* in the Cambodian Mekong River. *Fish. Sci.* **72**, 469–476.
- Soivio, A. and Tuurala, H.** (1981). Structural and circulatory responses to hypoxia in the secondary lamellae of *Salmo gairdneri* gills at two temperatures. *Comp. Biochem. Physiol. A.* **145**, 37–43.
- Sollid, J., Angelis, P. D., Gundersen, K. and Nilsson, G. E.** (2003). Hypoxia induces adaptive and reversible gross morphological changes in crucian carp gills. *J. Exp. Biol.* **206**, 3667–3673.
- Sollid, J., Weber, R. E. and Nilsson, G. E.** (2005). Temperature alters the respiratory surface area of crucian carp *Carassius carassius* and goldfish *Carassius auratus*. *J. Exp. Biol.* **208**, 1109–1116.
- Tuurala, H., Egginton, S. and Soivio, A.** (1998). Cold exposure increases branchial water–blood barrier thickness in the eel. *J. Fish Biol.* **53**, 451–455.

- Tzaneva, V., Gilmour, K. M. and Perry, S. F.** (2011). Respiratory responses to hypoxia or hypercapnia in goldfish (*Carassius auratus*) experiencing gill remodelling. *Respir. Physiol. Neurobiol.* **175**, 112-120.
- Wood, C. M. and Perry, S. F.** (1985). Respiratory, circulatory, and metabolic adjustments to exercise in fish. In *Circulation, Respiration, and Metabolism* (ed. R. Gilles), pp. 2-22. Berlin: Springer.
- Wood, C. M. and Randall, D. J.** (1973a). The influence of swimming activity on sodium balance in the rainbow trout (*Salmo gairdneri*). *J. Comp. Physiol. A.* **82**, 207-233.
- Wood, C. M. and Randall, D. J.** (1973b). The influence of swimming activity on water balance in the rainbow trout (*Salmo gairdneri*). *J. Comp. Physiol. A.* **82**, 257-276.
- Van Zalinge, N., Sopha, N. L., Bun, N. P., Kong, H. and Jørgensen, J. V.** (2002). Status of the Mekong *Pangasianodon hypophthalmus* resources, with special reference to the stock shared between Cambodia and Viet Nam. MRC Technical Paper No. 1, Mekong River Commission, Phnom Penh. 29 pp.
- Zheng, W. B. and Liu, W. S.** (1988). Morphology and histology of the swimbladder and infrastructure of respiratory epithelium in the air-breathing catfish, *Pangasius sutchi* (Pangasiidae). *J. Fish Biol.* **33**, 147-154.